On the Onset and Control of Chaos in Hysteretic Systems Using the Bouc–Wen Model

Abel Viji George
Department of Aerospace Engineering
Indian Institute of Technology Madras
ae21b001@smail.iitm.ac.in

1 Summary of the Original Paper

1.1 Introduction

The paper by Ngouoko et al. (2021) [1] investigates the appearance of horseshoe chaos in a single-degree-of-freedom (SDOF) nonlinear system with a hysteretic restoring force modeled using the Bouc–Wen formulation. The system incorporates negative stiffness elements [2], commonly referred to as 'anti-springs', which enhance energy dissipation by introducing a softening behavior into the system. Using Melnikov's method, the authors derive an analytical criterion for the onset of chaos under periodic forcing and validate their findings through numerical simulations. The study highlights how the shape parameters of the hysteresis function influence the emergence and suppression of chaos in the system, and demonstrates how the fractal nature of the basin of attraction boundaries appears with the onset of chaos and disappears when it is suppressed. In addition to identifying the critical forcing amplitude F_{CR}, the authors show that tuning the hysteretic parameters can effectively delay or prevent chaotic transitions.

1.2 Mathematical Modeling

The system under study is a single-degree-of-freedom (SDOF) oscillator with mass m, viscous damping c, and a restoring force composed of linear elastic and nonlinear hysteretic components, modeled using the Bouc–Wen formulation. The equation of motion under harmonic excitation is:

$$m\ddot{x}(t) + c\dot{x}(t) + H(x, z, t) = F(t) \tag{1}$$

where $x(t)$ is the displacement, and $H(x, z, t)$ is the total restoring force given by:

$$H(x, z, t) = \alpha k x(t) + k(1 - \alpha)z(t) \tag{2}$$

Here, k is the linear stiffness, and α is the post-yield to pre-yield rigidity ratio. The hysteretic variable $z(t)$ is governed by the Bouc–Wen differential model [3]:

$$\dot{z} = \frac{1}{D}\left(A\dot{x} - \beta|\dot{x}||z|^{n-1}z - \gamma\dot{x}|z|^{n}\right) \tag{3}$$

Parameters $A > 0$, β, γ, and $n > 1$ control the shape of the hysteresis loop. The hysteresis behavior is thermodynamically admissible if $\beta \geq \gamma$. The combination of β and γ determines whether the loop is softening or hardening. Figure 1 illustrates these behaviors. The external excitation is assumed harmonic: $F(t) = F_0 \sin(\Omega t)$, where F_0 and Ω are the forcing amplitude and frequency, respectively. The governing equation can be rewritten as:

$$\ddot{x}(t) + 2\zeta\omega\dot{x}(t) + \alpha\omega^2 x(t) + \omega^2(1 - \alpha)z(t) = F(t) \tag{4}$$

with natural frequency $\omega = \sqrt{k/m}$ and damping ratio $\zeta = \frac{c}{2m\omega}$. The evolution of the hysteretic displacement z given by the following constitutive differential equation:

$$\dot{z} = \frac{1}{D}\left[A - (\gamma + \varepsilon\beta)|z|^n\right]\dot{x}, \quad \varepsilon = \mathrm{sgn}(\dot{x})\,\mathrm{sgn}(z) \tag{5}$$

This model captures the essential nonlinear hysteretic dynamics, enabling analytical and numerical exploration of chaotic behavior under periodic excitation.

1.3 Appearance of Separatrix and Melnikov Analysis

The system dynamics from equations (4) and (5) can be recast in state-space form for an unperturbed system with no external forcing:

$$\begin{aligned} \dot{x} &= y \\ \dot{y} &= -2\zeta y - \alpha\omega^2 x - (1-\alpha)\omega^2 z \\ \dot{z} &= D^{-1}\left[A - (\gamma + \varepsilon\beta)|z|^n\right] y \end{aligned} \tag{6}$$

For $D = 1$ and $n = 2$, one obtains three fixed points:

$$(0,\ 0,\ 0), \quad \left(-\frac{(1-\alpha)}{\alpha}\sqrt{\frac{A}{\gamma+\varepsilon\beta}},\ 0,\ \sqrt{\frac{A}{\gamma+\varepsilon\beta}}\right), \quad \left(\frac{(1-\alpha)}{\alpha}\sqrt{\frac{A}{\gamma+\varepsilon\beta}},\ 0,\ -\sqrt{\frac{A}{\gamma+\varepsilon\beta}}\right)$$

Taking into account the influence of the hysteretic force, the potential energy of the system is given by:

$$V(x) = \frac{1}{2}\alpha\omega^2 x^2 + \omega^2(1-\alpha)\int_{x(0)}^{x(t)} z\,dx \tag{7}$$

It is claimed that the hysteretic displacement can be derived explicitly with the assumption of $x(0) = 0$, $\dot{x}(0) = 0$ and $z = 0$ and is given by:

$$z = \frac{\sqrt{A}}{\sqrt{\gamma+\varepsilon\beta}}\tanh\left(\sqrt{A(\gamma+\varepsilon\beta)}\,x\right) \tag{8}$$

It is not possible to continue the analytical discussion using the complicated term in equation (8). For small shape parameters β and γ, a quartic approximation of the potential is used:

$$V_{\text{ap}}(x) = \frac{1}{2}K_1 x^2 - \frac{1}{12}K_3 x^4 \tag{9}$$

where K_1 and K_3 depend on α, A, γ, β, and ω. This potential leads to a monostable structure with heteroclinic orbits and this has been shown in Figure 2a. The appearance of the separatrix is indicative of the intersection of the perturbed and unperturbed heteroclinic orbits. This intersection suggests the onset of horseshoe chaos. So, the shape parameters of the hysteresis force have a direct link with the appearance of horseshoe chaos in the system.

Melnikov Analysis is an effective method to analytically compute the threshold for the onset of horseshoe chaos in the Bouc-Wen model. The Melnikov function [4] is:

$$M(\tau_0) = -2\zeta\omega\int_{-\infty}^{+\infty} y_{\text{het}}^2(\tau)\,d\tau + F_0\int_{-\infty}^{+\infty} y_{\text{het}}(\tau)\sin(\Omega(\tau+\tau_0))\,d\tau \tag{10}$$

where, (x_{het}, y_{het}) are the pair of saddle points which form the heteroclinic orbit. Horseshoe Chaos occurs when $M(\tau_0)$ has simple zeros. This yields a threshold condition for the forcing amplitude:

$$F_0 \geq F_{\text{CR}} = \left|\frac{4\zeta\omega^3\left(\alpha + (1-\alpha)A\right)^2}{(\gamma+\varepsilon\beta)(1-\alpha)A^2\,\Omega\pi\sin(\Omega\tau_0)}\sinh\left(\frac{\Omega\pi}{2\omega\sqrt{\frac{\alpha+(1-\alpha)A}{2}}}\right)\right| \tag{11}$$

2 Replicated Results

The shape parameters of the Bouc-Wen model determines the strain-softening behaviour of the hysteresis loops. When $\beta + \gamma > 0$, the hysteresis loop shows a strain-softening behaviour and when $\beta + \gamma < 0$, it shows a strain-hardening behaviour as seen in Figure 1.

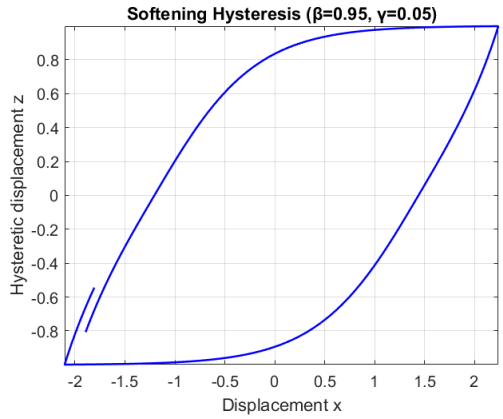

(a) Softening hysteresis loop generated by the model for $D = 1$, $n = 2$, $A = 1$, $\gamma = 0.05$ and $\beta = 0.95$

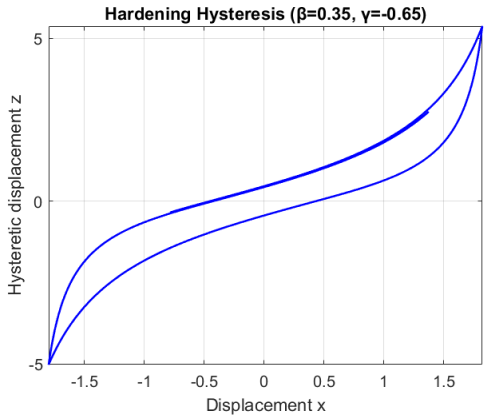

(b) Hardening hysteresis loop generated by the model for $D = 1$, $n = 2$, $A = 1$, $\gamma = -0.65$ and $\beta = 0.35$

Figure 1: Strain-softening and hardening behaviour depending on the sign of $\beta + \gamma$

The potential energy of the system, after the quartic approximation as shown in Figure 2a shows the monostable nature of the system with one stable Fixed point and two unstable fixed point. Figure 2b shows the heteroclinic orbit for the unperturbed system.

Since we have an analytical expression for (11), we can see how F_{CR} varies with some parameters. Two

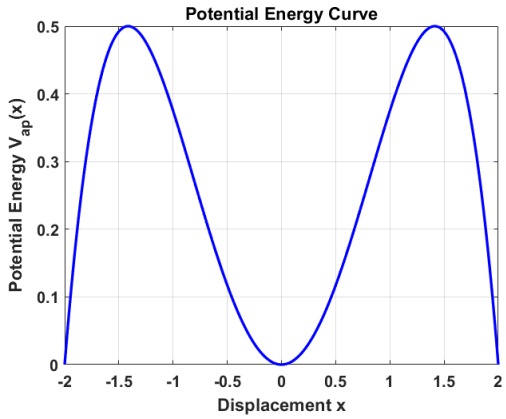

(a) Potential Energy for the unperturbed system

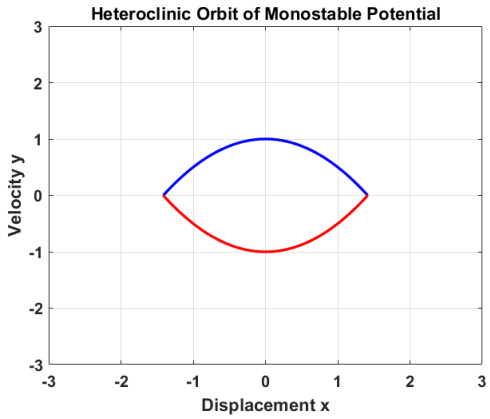

(b) Heteroclinic orbit for the unperturbed system

Figure 2: Potential Energy Curve and heteroclinic orbit for the unperturbed case

examples are shown in Figure 3.

Conventional basin boundary studies typically employ two distinct colors in scatter plots to differentiate regions of stability—one color representing decaying, stable trajectories and another indicating diverging, unstable behavior [5]. A slightly different approach is followed in this report and will be discussed in the next section.

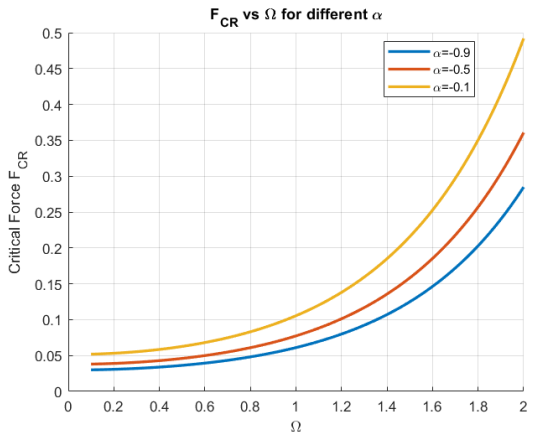

(a) F_{CR} vs Ω for different α

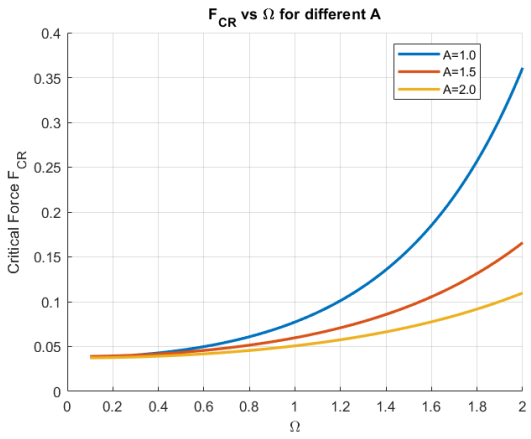

(b) F_{CR} vs Ω for different A

Figure 3: Dependency of F_{CR} on some parameters of the Bouc-Wen model

3 Novel Results

A fundamental characteristic of the Melnikov theory is the fractality of the basin of attraction when chaos is present. In [1] the focus is on the amplitude of the external forcing as our parameter to study the onset of chaos. There are always two sets of parameters considered:

- Uncontrolled: $\epsilon = 1$, $\alpha = -0.5$, $\beta = 0.95$, $\gamma = 0.05$, $\zeta = 0.02$ and $A = 1$.
- Controlled: $A = 0.7$, $\alpha = -0.4$, $\gamma + \epsilon\beta = 0.9$ with other parameters same as the uncontrolled case.

To visualize the sensitive dependence on initial conditions and identify chaotic regions, the Basin of Attraction(BoA) was computed via a grid-based simulation. The phase space was sampled over a fine 200×200 grid of initial positions and velocities, with each trajectory numerically integrated over time using MATLAB's stiff ODE solver `ODE15s` [6]. Trajectories were classified as bounded or unbounded based on final displacement and convergence rate. A color-coded map was generated by assigning values based on stabilization time or escape behavior and normalized over a continuous color scale. The highest values (reddish color) corresponds to the most unstable and the lowest values (bluish color) is for stable initial conditions. The resulting plot in Figure 4 reveals fractal-like boundaries between stable and unstable regions, indicating the presence of horseshoe chaos. The critical forcing amplitude was computed using (11) and was found to be $F_{CR} = 0.0773$.

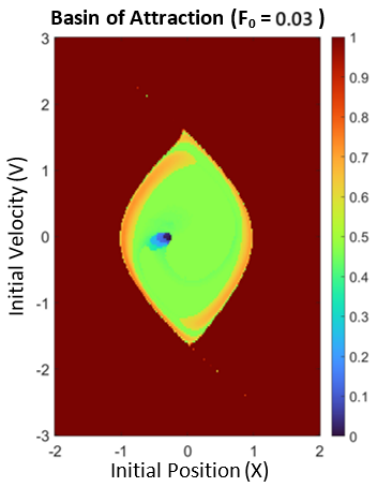

(a) Uncontrolled case, $F_0 < F_{CR}$ showing a well defined geometry for the BoA.

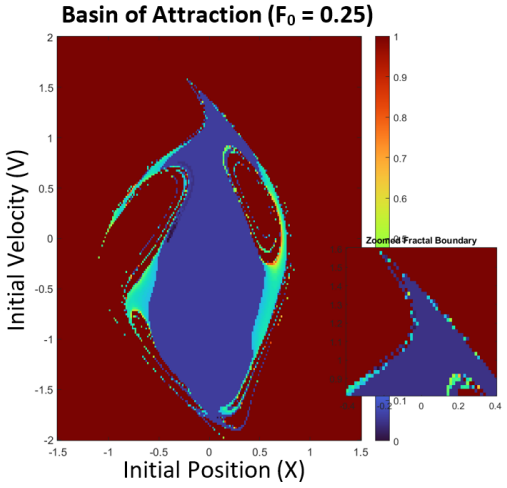

(b) Uncontrolled case, $F_0 > F_{CR}$, showing the fractal nature of the basin boundaries, suggesting chaos.

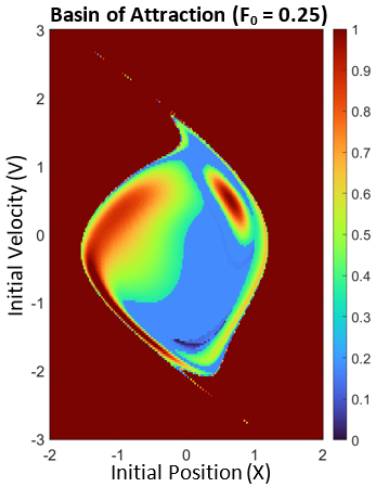

(c) Controlled case, $F_0 > F_{CR}$, showing a well defined geometry for the BoA.

Figure 4: Showing how the onset of chaos can be controlled by varying the parameters of the Bouc-Wen model.

Inspired by classical examples like the Lorenz attractor, it can be checked whether this system exhibits similarly complex behavior by plotting the $3D$ phase trajectory for the x, $\dot{x}$, z. Figure 5 compares trajectories for the uncontrolled cases with $F_0 < F_{\text{CR}}$ and $F_0 > F_{\text{CR}}$. It can be seen that the trajectories remain confined to a bounded region similar to the Lorenz case. A notable difference from the Lorenz case [5] is to be expected because this is a system with only one stable fixed point, ruling out the existence of strange attractors unlike the Lorenz case with two stable fixed points. Notably, the controlled case with $F_0 > F_{\text{CR}}$ (not shown here) visually resembles the stable $F_0 < F_{\text{CR}}$ case, suggesting suppression of chaotic dynamics.

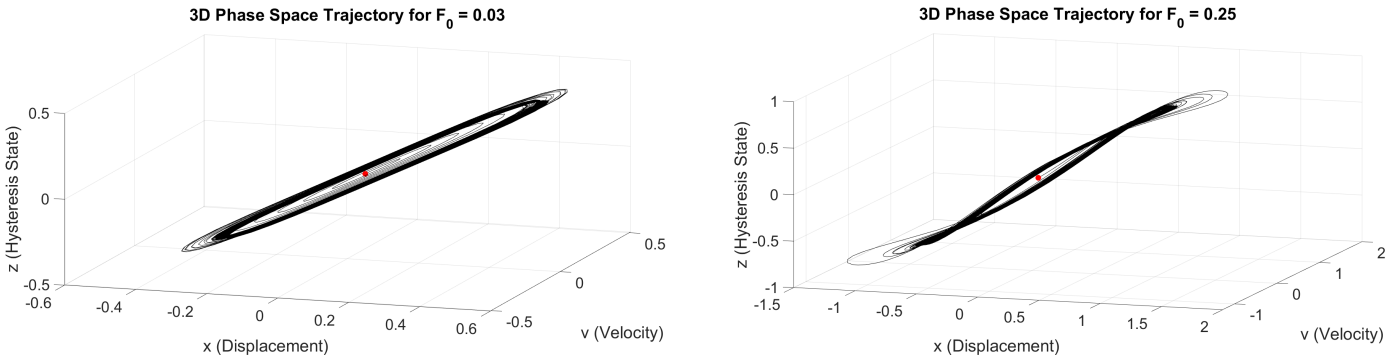

(a) $F_0 = 0.03$, uncontrolled (b) $F_0 = 0.25$, uncontrolled

Figure 5: Comparing the $3D$ phase trajectories for the cases with and without chaos.

A Poincaré section is used to study the system's response over periodic intervals. Figure 6 shows that for $F_0 < F_{\text{CR}}$, trajectories converge to a single point—indicating a limit cycle. For $F_0 > F_{\text{CR}}$, the section reveals a scattered set of points with no apparent periodicity, suggesting chaotic behavior. However, due to lack of clarity, this alone is not conclusive. Interestingly, zoomed views of the Poincaré map reveal self-similar patterns, a feature often associated with chaos [7].

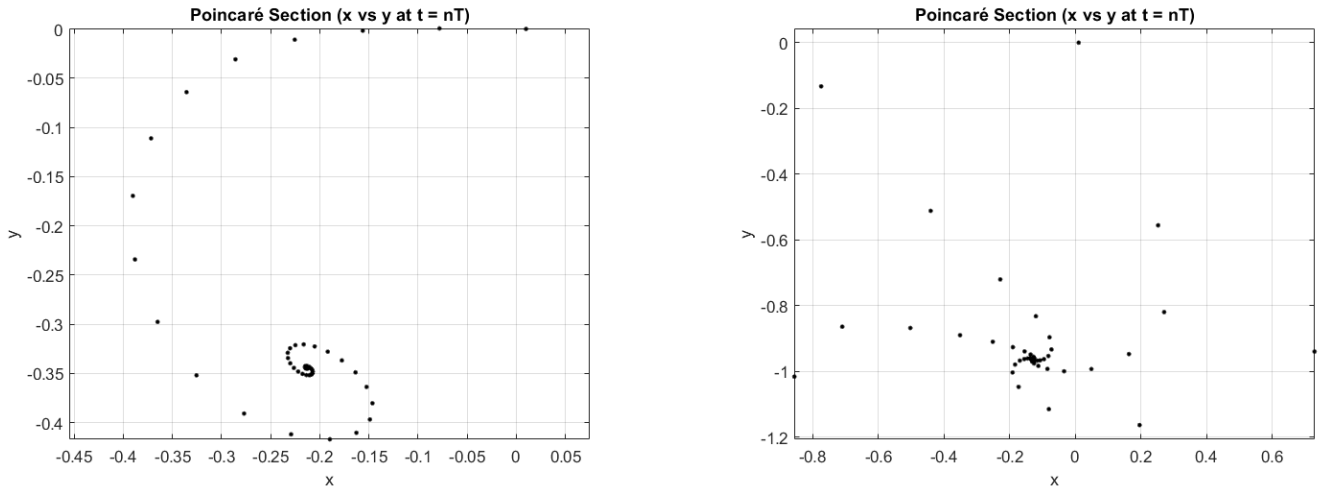

(a) $F_0 = 0.03$, uncontrolled (b) $F_0 = 0.25$, uncontrolled

Figure 6: Comparing the $3D$ phase trajectories for the cases with and without chaos.

Finally, Lyapunov exponents are computed for three cases and shown in Figure 7. These plots illustrate the evolution of the separation $\delta(t)$ between initially close trajectories. The exponent is nearly zero for the non-chaotic cases (uncontrolled $F_0 < F_{\text{CR}}$ and controlled $F_0 > F_{\text{CR}}$), while it is positive for the uncontrolled $F_0 > F_{\text{CR}}$ case—clearly indicating chaotic behaviour. This confirms that control via parameter tuning can effectively suppress chaos. It is important to note that the magnitudes depend on the time interval considered. It is expected to have an initial transience and a final leveling off. The trajectories cannot diverge to infinity as they entire $3D$ space is confined to a particular finite region as expected from the Lorenz attractor case.

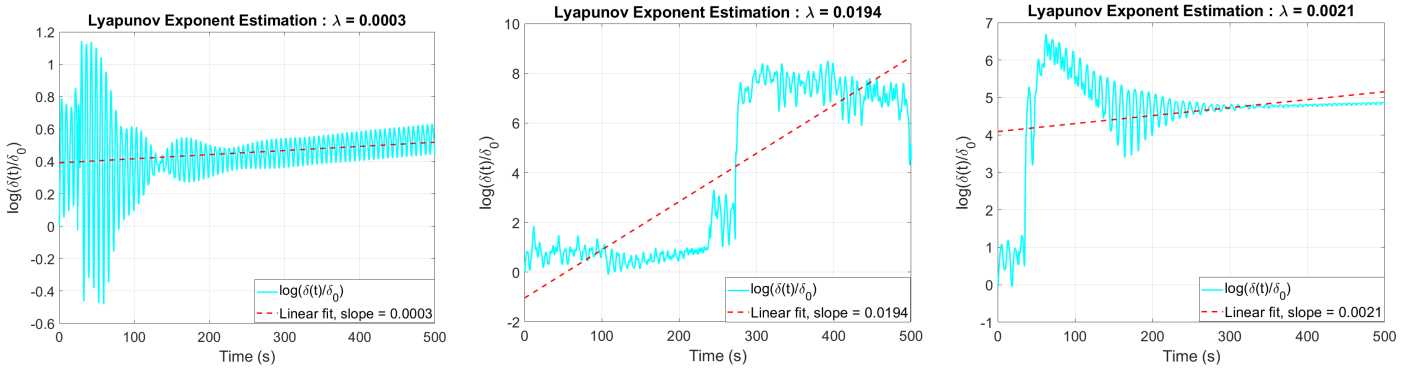

(a) Uncontrolled case, with $F_0 < F_{CR}$ (b) Uncontrolled case, with $F_0 > F_{CR}$ (c) Controlled case, with $F_0 > F_{CR}$

Figure 7: Lyapunov Exponent plots showing how the onset of chaos can be controlled by varying the parameters of the Bouc-Wen model.

4 Conclusion

This study explored the onset and control of chaos in a nonlinear hysteretic system governed by the Bouc–Wen model with negative stiffness. Using both analytical tools such as Melnikov analysis and numerical techniques, the dynamic response of the system was thoroughly investigated. It was shown that the shape parameters of the hysteresis function have a direct influence on the appearance of horseshoe chaos. The derived analytical threshold for chaotic motion, F_{CR}, served as a useful predictor for the onset of chaotic dynamics under harmonic excitation. Through extensive MATLAB simulations, the fractal nature of the basin of attraction was clearly observed when the forcing amplitude exceeded this critical value. Additionally, the system's behaviour was visualized using conventional chaos diagnostics. The Lyapunov exponent analysis confirmed that chaos could be mitigated or entirely suppressed by tuning the hysteretic parameters — effectively demonstrating a mechanism for controlling nonlinear instability.These findings reinforce the importance of hysteretic parameter design in structural and mechanical systems where chaos may pose safety or performance concerns. Future work may involve exploring in depth the self-similar nature of the Poincaré sections and understanding if there are specific patterns formed in the phase trajectories similar to the Lorenz strange attractors. Another route to pursue would be to check if chaos can be controlled by varying other parameters of the model apart from the forcing amplitude as was done in this study.

References

[1] O. N. Y. Ngouoko, B. R. Nana Nbendjo, and U. Dorka, "On the appearance of horseshoe chaos in a nonlinear hysteretic systems with negative stiffness," *Archive of Applied Mechanics*, vol. 91, no. 11, pp. 4621–4630, 2021.

[2] C. Geo and E. Charalampakis, "A new hysteretic nonlinear energy sink (hnes)," *Communications in Nonlinear Science and Numerical Simulation*, vol. 60, pp. 1–11, 2018.

[3] F. Ikhouane and J. Rodellar, "On the hysteretic bouc-wen model. part i: Forced limit cycle characterization," *Nonlinear Dynamics*, vol. 42, pp. 63–78, 2005.

[4] S. Wiggins, *Introduction to Applied Nonlinear Dynamical Systems and Chaos*. New York: Springer, 1990.

[5] S. H. Strogatz, *Nonlinear Dynamics and Chaos: With Applications to Physics, Biology, Chemistry, and Engineering*. Reading, Massachusetts: Perseus Books, 1994.

[6] A. V. George, "Github repository for the codes," https://github.com/Flerovium-114/AM5650_Course_Project, 2025.

[7] A. Shahhosseini, M.-H. Tien, and K. D'Souza, "Poincaré maps: a modern systematic approach toward obtaining effective sections," *Nonlinear Dynamics*, vol. 111, pp. 529–548, 2023.